ARTICLE IN PRESS

OPEN ACCESS

Journal of Multidisciplinary Applied Natural Science Vol. xx No. xx (xxxx) https://doi.org/10.47352/jmans.2774-3047.429

Check for updates

Research Article

PVA/ZnO-Modified Bacterial Cellulose Acetate Membranes from Pineapple Peel Waste with Improved Thermal Stability, Antibacterial, and Filtration Performance

Uun Yanuhar, Heru Suryanto*, Joseph Selvi Binoj, Leong-Seng Lim, Arumugam Kumaravel, Aminnudin Aminnudin, Fajar Nusantara, Defa Rizqi Machfuda, Komarudin Komarudin, and Aulia Surya Ramadhan

Received : November 12, 2025 | Revised : February 11, 2026 | Accepted : April 20, 2026 | Online : May 7, 2026

Abstract

The purpose of this work is to create and assess bacterial cellulose acetate (BCA) membranes reinforced with zinc oxide (ZnO) nanoparticles and mixed with polyvinyl alcohol (PVA). BCA membranes were made from pineapple peel biowaste and they contain 0.25 wt.% ZnO and PVA at 2.5 wt.% and 5.0 wt.%. Fourier-transform infrared spectroscopy, scanning electron microscopy, and X-ray diffraction (XRD) were used to observe the properties of membrane structure. Thermogravimetric analysis was used to examine the developed membrane's thermal degradation. Additionally, the filtration capabilities and antibacterial activity were examined. Furthermore, the membrane's morphology demonstrates that the addition of PVA results in denser surfaces, and ZnO was distributed without substantially changing the fiber's morphology. Similarly, the XRD analysis shows that as the PVA content increases, the crystallinity index decreases and the crystallite size slightly increases. Moreover, the thermal analysis demonstrated that PVA improves membrane stability by reducing the rate of mass loss. The PVA has a minor impact on antibacterial activity against *Staphylococcus aureus* and *Escherichia coli*. However, it appears that the ZnO content in the membrane was the source of the antibacterial activity. Besides, the brackish water filtration test revealed that the addition of PVA at 2.5 wt.% and 5.0 wt.%, respectively, enhanced the efficacy of bacterial filtration by 17.9 and 10.7 times. These results demonstrate that PVA/ZnO-modified BCA membranes are viable, environmentally friendly options for sustainable aquaculture and water filtration systems.

Keywords: antibacterial activity, bacterial cellulose acetate, membrane filtration, polyvinyl alcohol, ZnO nanoparticles

1. INTRODUCTION

Developing technologies for cellulose production is a key priority to valorize the biomass and agricultural residues into high-value products. Cellulose is an abundant material with a production of about 1.5 trillion tons annually [1], equal to USD 144.21 billion in 2024 [2]. It is an attractive material due to its sustainability, high purity, and excellent mechanical properties [3]. However, increasing the cellulose consumption contributes to deforestation, which contributes to environmental degradation. So, agricultural biowaste is a viable cellulose source offering a sustainable alternative.

Indonesia is a producer country of pineapple (*Ananas comosus*) with around 3.16 billion tons in 2023 [4]. Also, the waste rose from a poor post-harvest is up to 55% waste, which can cause pollution [5]. Valorization of this waste can be done by a bioconversion process to transform biowaste into fuels [6]. Another route is utilizing this waste extract for bacterial cellulose (BC) production, then applying it as aerogels for dye adsorption [7], and membranes for wastewater treatment [8]. However, the performance of BC membranes depends on culture conditions [9], pretreatment [10], homogenization [11], and reinforcement with nanomaterials [12].

Cellulose acetate (CA), a derivative obtained by acetylating hydroxyl groups of cellulose, is widely applied for membrane fabrication due to its low cost, easy processing, and wide availability [13]. Still, improvements in permeability, salt rejection, thermal resistance, and strength are required for CA membranes to compete with film composites. Incorporating nanomaterials is a common strategy: multi-walled carbon nanotubes enhance separation [14], Titanium dioxide (TiO_2) for increasing the membrane strength [15], silver nanoparticles improve water treatment [16], and Iron(III) oxide (Fe_3O_4) provides potential in packaging sectors [17]. Zinc oxide (ZnO) nanoparticles have potential due to their abundance, antibacterial activity, and

Please cite this article as: U. Yanuhar, H. Suryanto, J. S. Binoj, L.-S. Lim, A. Kumaravel, A. Aminnudin, F. Nusantara, D. R. Machfuda, K. Komarudin, and A. S. Ramadhan. (2026). "PVA/ZnO-Modified Bacterial Cellulose Acetate Membranes from Pineapple Peel Waste with Improved Thermal Stability, Antibacterial, and Filtration Performance". *Journal of Multidisciplinary Applied Natural Science*. https://doi.org/10.47352/jmans.2774-3047.429

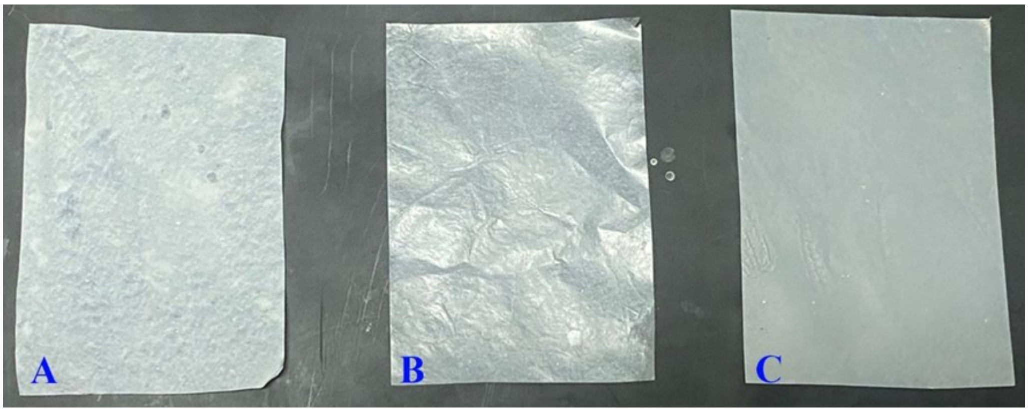

Figure 1. Product of membrane synthesis: (A) BCA control; (B) BCA/ZnO (0.25 wt.%)/PVA 2.5 wt.%; and (C) BCA/ZnO (0.25 wt.%)/PVA 5.0 wt.%.

reinforcement potential [18][19]. ZnO inhibits bacterial growth through Zn^{2+} ions and reactive oxygen species that causes membrane damage [20].

Effective water filtration is the process to maintain water quality and to protect ecosystem health and stability by removing contaminants and pathogens [21][22]. Previous sstudies had reported the utilization of natural materials such as banana peel, cassava peel, and coconut husk [22], and orange peel powder [23] as a membrane for removing the contaminant. Utilizing pineapple biowaste has benefits for both environmental management as well as production of cost-effective green materials. Meanwhile, inefficient waste disposal can pose health and ecological risks, with mitigation often exceeding the costs of proper waste management systems.

The bacterial cellulose membranes are known to be studied for water purification [24][25]. Drawbacks of cellulose as a membrane are poorer barrier properties against moisture [26], low chemical resistance, and poor mechanical strength [27]. It should be improved through crosslinking [28], blending [29], surface modification [30] and by making a composite [31]. Polyvinyl alcohol (PVA) is a water-soluble polymer with abundant –OH groups that potential to form strong hydrogen bonds with cellulose fibers. Blending PVA with BC is very important to increase mechanical strength, flexibility, and water retention [32][33], so that it can overcome the limitations of cellulose membranes.

Although ZnO nanoparticles have been extensively studied, their effects on cellulose-based membranes, particularly cellulose acetate membranes, show inconsistent results [34][35]. Previous study showed that addition of ZnO reduce the mechanical properties of bacterial cellulose membrane [36]. Furthermore, while PVA is commonly used to enhance mechanical and water retention properties, the molecular interactions between ZnO nanoparticles and PVA in cellulose acetate matrices are not fully elucidated. They can vary depending on the synthesis conditions and component ratios [37]. These gaps highlight the need to systematically investigate how blending PVA with ZnO nanoparticles affects membrane structure, mechanics, antibacterial behavior, and filtration efficiency. Therefore, the present study membranes from cellulose acetate derived from pineapple waste was fabricated, blended with varying concentrations of PVA and ZnO nanoparticles reinforcement, aiming to clarify the role of PVA concentration on the resulting excellent membrane properties.

2. MATERIALS AND METHODS

2.1. Materials

Pineapple biowaste was obtained from the Blitar Regency, Indonesia. ZnO nanoparticles have a size ranging from 20 to 30 nm, supplied by Hongwu Materials, China. PVA was supplied by Himedia (India). Other reagents used for the fermentation process to produce BC, including NaOH and NH_3, were purchased from Loba Chemie (India), urea was supplied from Kanto Chemical (Japan), CH_3COOH was purchased from Smart Lab (India), and glucose was provided by Lansida (Indonesia).

2.2. Methods

2.2.1. Production of BC Suspension

Biosynthesis of BC was conducted using pineapple peel extract. A 2 L of extract was added with 200 g of glucose, 10 g of ammonia, while the pH was maintained at 4.5. The added glucose served as the primary energy and carbon source for bacterial metabolism, ensuring optimal biosynthesis of the cellulose network and consistent pellicle yield from the pineapple waste medium. Medium was added with 200 mL *Acetobacter xylinum* (Indahasco, Indonesia), then held at 25–30 ˚C. After 14 days, the BC pellicle that floated on medium was collected and washed until the pH was neutral. Pellicle was boiled in an alkali (NaOH) solution of 6% for 2 h, then rinsed until neutral. Pellicle was cut into small pieces, put into the blender chamber (Fomac, Indonesia) containing 250 mL water, then the bacterial cellulose was crushed for 5 min in three consecutive cycles to obtain a fine suspension. Homogenization process followed Mahsuli *et al*. methods [38] at 150 bar for 5 cycles in High-Pressure Homogenizer (AH-100D, Berkley Scientific, China).

2.2.2. Synthesis of Bacterial Cellulose Acetate-Based Membrane

Bacterial cellulose acetate (BCA) derived from BC was used as the base material. BCA preparations refer to the previously published methods [39]. The synthesis involves preparing BCA from 5 g of slurry BC. Also, the PVA was prepared by dissolving the polymer in distilled water at 80 ˚C under continuous stirring until a clear solution was obtained, then cooled to room

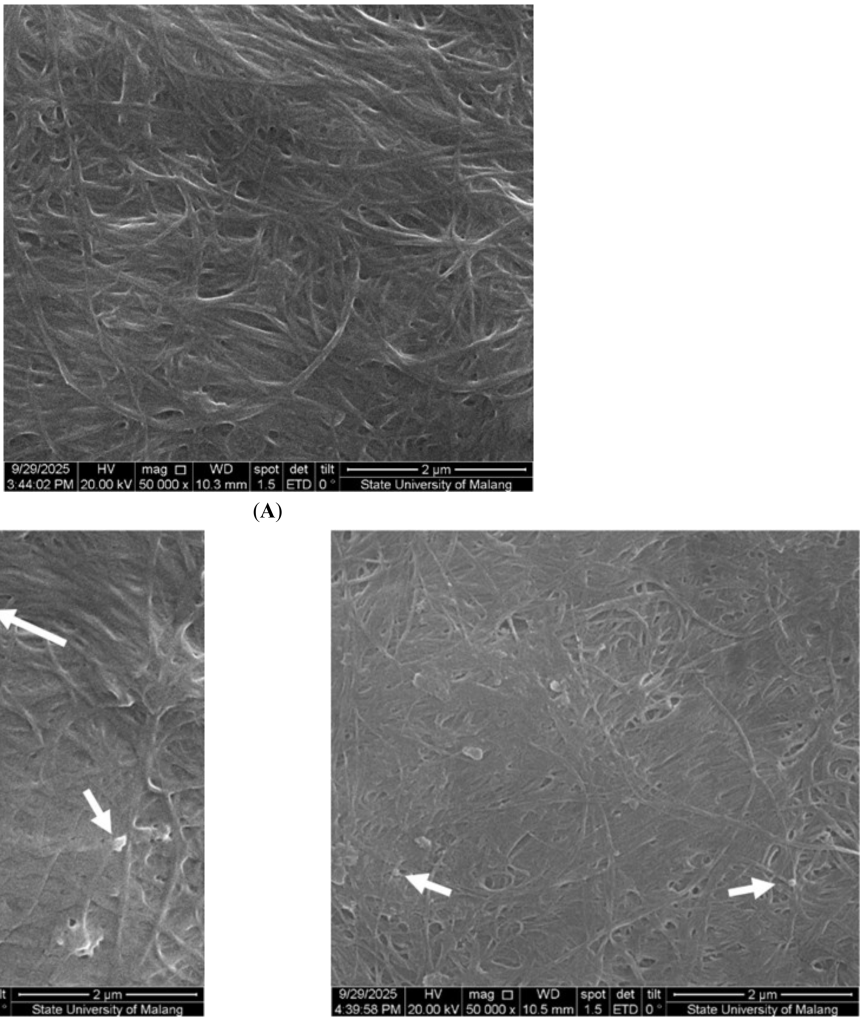

(A)

(B)

(C)

Figure 2. Surface morphology of BCA membrane: (A) BCA control; (B) BCA/ZnO (0.25 wt.%)/PVA 2.5 wt.%; and (C) BCA/ZnO (0.25 wt.%)/PVA 5.0 wt.%.

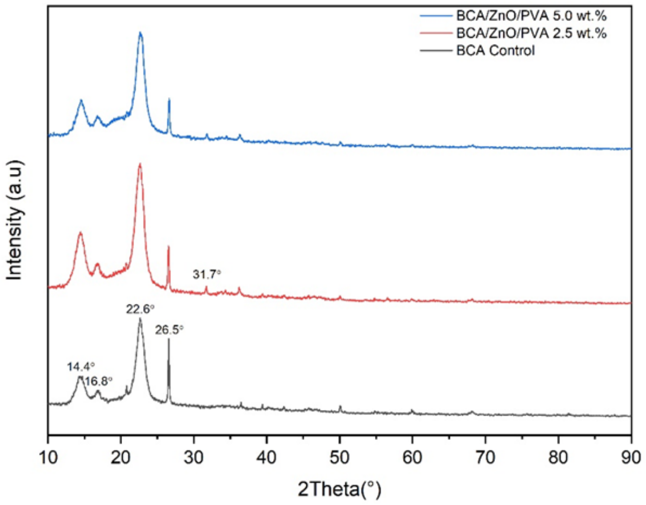

Figure 3. Diffractogram of hybrid BCA/ZnO membrane with PVA addition.

temperature (25˚C). Likewise, the two formulations were prepared using PVA concentrations of 2.5% and 5.0% (w/w) from 5 g of BC. A ZnO nanoparticle dispersion (0.25 wt% relative to 5 g of BC) was separately prepared in distilled water and sonicated (Lawson, China) with power 400 W for 15 min to prevent agglomeration. The higher concentrations of ZnO have an impact on membrane properties [40]. In addition, the PVA solution was gradually blended into the BCA suspension under magnetic stirring, followed by addition of ZnO dispersion. The resulting mixture was further homogenized by stirring and mild sonication to ensure uniform distribution of ZnO within the BCA/ PVA matrix. Finally, the homogeneous suspension was cast onto glass plates dies and dried in a dehydrator (Kris, Indonesia) at 60 ˚C for 24 h to obtain stable composite membranes.

2.2.3. Characterization Studies

The surface morphology of membranes was examined using a scanning electron microscope (SEM, FEI Inspect-S50, Japan) after sputter-coating with a thin 10 nm layer of gold using an Emitech coating unit (England). The crystalline structure was characterized on membrane samples prepared in 20 cm² sections using X-ray diffraction (XRD, PanAnalytical-X'Pert Pro, USA). Measurements were carried out in the 2θ range from 5˚ to 50˚ employing CuKα radiation (λ = 1.542 Å) at an operating current of 30 mA and a voltage of 40 kV. Crystalline index (CI) and crystallite size (L) were calculated using Equations (1) and (2) [41], respectively;

$$CI = \frac{I_{22} - I_{18}}{I_{22}} \times 100\% \qquad (1)$$

$$L = \frac{K\lambda}{\beta \cos\theta} \qquad (2)$$

where, I_{22} is the highest intensity at diffraction angle (θ) of around 22.0˚ and I_{18} is the lowest intensity at θ around 18˚. K is 0.89; θ is the diffraction angle; β is the full width at half-maximum/FWHM (rad.); λ is the x-ray wavelength.

Fourier-transform infrared (FTIR) spectra were recorded using a Shimadzu Prestige-21 spectrometer (Japan). However, prior to analysis, membrane samples were oven-dried at 105˚C for 3 h, ground into fine powder, and subsequently mixed with KBr at a ratio of 0.1 mg sample to 1.0 mg KBr. Later, the mixture was pressed into pellets and observed over the wavenumber range of 400–4000 cm^{-1} with a resolution of 2 cm^{-1}. Moreover, the thermal degradation analysis was conducted using Simultaneous Thermal Analyzer (STA 6000, USA) from 25 to 800 ˚C, with a temperature rate of 10 ˚C/ min. Mechanical properties was evaluate using tensile tester (TechnoLab, Indonesia) with maximum load of 50 N with five replication for each treatment.

2.2.4. Antibacterial Activity

The antibacterial performance of membranes was assessed using the agar disk diffusion technique against Gram-negative *Escherichia coli* (ATCC 25922) and Gram-positive *Staphylococcus aureus* (ATCC 23235) obtained from Hope Biotechnology, Shandong, China. Membrane discs (5 mm diameter) were tested, with chloramphenicol (3.0 mg/mL, Abbexa, USA) serving as the control (+) and CA membranes as the blank control. BCA membrane and membrane containing PVA 2.5 wt.% and 5.0 wt.% with ZnO 0.25 wt.% were denoted as samples I, II, and III respectively. Meanwhile, prior to testing, membranes were sterilized by heat treatment and ultraviolet C exposure. Also, the Mueller-Hinton agar (Oxoid, UK) was placed into the discs and inoculated with bacterial cultures. Further, the disk was then incubated at 36 ˚C for 24 h. Besides, each test was performed in triplicate and statistically analyzed using one-way ANOVA (significance level of 95%) followed by Tukey’s post-hoc test with Origin v.9 software.

2.2.5. Filtration Performance

The bacterial filtration effectiveness was evaluated on 500 mL of brackish water. Water sample was collected in the estuary region in Pasuruan Regency, East Java, Indonesia. The brackish water was filtered through the membranes mounted in syringe barrels. Also, the permeates were used to grow the bacteria by culturing the filtrates on agar plates using the pour plate technique, followed by colony counting to determine the abundance of bacteria. The bacterial filtration effectiveness was calculated by log reduction value (LRV), as shown in Equation (3) [42];

$$LRV = Log_{10}\left(\frac{Ni}{Nf}\right) \tag{3}$$

where, Ni is bacterial abundance in control and Nf is bacterial abundance in treatment.

3. RESULTS AND DISCUSSIONS

3.1. Morphology of BCA/ZnO/PVA Membrane

Synthesis of the BCA membrane with the addition of ZnO and PVA is depicted in Figure 1. Figure 1(a) (BCA control) shows a slightly opaque surface with an uneven texture and several fine spots, indicating a non-homogeneous component distribution and the possible presence of small pores due to the absence of a reinforcing additive. Figure 1(b) (BCA/ZnO(2.5 wt.%)/PVA 2.5 wt.%) displayed that the addition of ZnO and PVA resulted in a slightly wrinkled and uneven surface, thereby leads to an improved membrane structure. Meanwhile, Figure 1(c) (BCA/ZnO(2.5 wt.%)/PVA 5.0 wt.%) exhibited the smoothest, densest, and glossiest surface with minimal defects, indicating a more homogeneous and compact structure. These differences in morphological characteristics indicates that varying the concentrations of PVA significantly impacts the homogeneity, compactness, and surface quality of the resulting membrane.

The morphology of membrane surface observed under SEM is depicted in Figure 2. The BCA membrane (Figure 2(a)) exhibits a smooth, random, and homogeneous fiber structure, representing the original characteristics of BCA and no inorganic particles were found on the surface. In the BCA/ZnO (0.25 wt.%)/PVA 2.5 wt.% membrane (Figure 2(b)), the fibril structure is still clearly visible, but there is a change in texture due to the addition of PVA. Also, the PVA acts as a binding agent that increases the interfiber bond, resulting in a slightly denser surface than pure BCA. In addition, the ZnO nanoparticles at a concentration of 0.25 wt.% are identified as bright spots (indicated by arrows), their number is relatively small and does not dominate the surface morphology. Meanwhile, in the BCA/ZnO (0.25 wt.%)/PVA 5.0 wt.%

Table 1. Structure of BCA membrane observed by XRD pattern.

Sample	Intensity of diffraction angle			L	CI
	14.4	18	22.6	(nm)	(%)
BCA	241	92	577	8.58	84.06
BCA/ZnO (2.5 wt.%)/ PVA2.5wt.%	424	160	827	8.60	80.65
BCA/ZnO (2.5 wt.%)/ PVA5.0wt.%	299	142	693	9.36	79.51

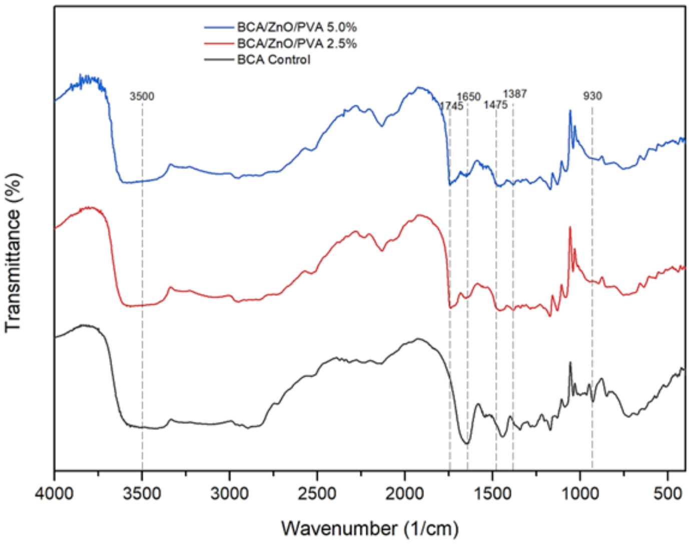

Figure 4. Spectrogram for BCA and BCA/ZnO(2.5 wt.%)/PVA with content of 2.5 wt.% and 5.0 wt.%.

Table 2. Analysis on functional groups of BCA/ZnO/PVA membrane.

No.	**PVA Concentrations (wt.%)**			**Assignment**
	Control	**2.5**	**5.0**	
1	3500	3500	3500	O–H stretching [56]
2	-	1745	1745	C=O Stretching [57]
3	1650	1650	1650	OH bending [58]
4	1446	1475	1475	CH_2 bending vibration [59][60]
5	-	1387	1387	O–H bending [61][62]
6	930	-	-	C–O stretching [63][64]

membrane (Figure 2(c)), the effect of PVA is more obvious. Higher PVA additions cause some of the fibril network to appear covered by a thin layer, making the surface appear smoother and denser. On the other hand, the fiber structure became less clearly defined, and the gaps between the fibers decreased. Overall, changes in membrane surface morphology were more influenced by the addition of PVA, while ZnO at low concentrations (0.25 wt.%) only acted as dispersed particles without causing significant changes in fiber shape.

Morphology of the membrane surface changes due to addition of PVA owing to a direct impact on the physical and functional properties of membrane. Meanwhile, pure BCA membranes, which have an open fibril structure with greater porosity, have the potential to provide high water permeability, but tend to be less stable [43]. In the BCA/ZnO (0.25 wt.%)/PVA 2.5 wt.% membrane, better inter fiber bonding results in a denser surface structure than the pure membrane, thereby the water permeability is slightly reduced. However, the presence of PVA at this moderate concentration actually increases the mechanical strength of the membrane because the fibers are more tightly bound and the load distribution is more even [44]. At a higher PVA concentration (5.0 wt.%), the surface morphology becomes smoother, denser, and most of the open pores are closed. This condition has the potential to significantly reduce water permeability, but simultaneously increases the density and mechanical strength of membrane [45]. In addition, the ZnO dispersion is maintained, but its main contribution is more into antibacterial function than to morphological effects [46]. Thus, the addition of PVA plays a dominant role in controlling the balance between permeability and mechanical strength of the membrane, while ZnO, even in low amounts, still provides additional functions in the form of antibacterial properties. Therefore, it was observed that the selection of PVA concentration is a key factor in optimizing the performance of BCA/

ZnO-based membranes.

3.2. Membrane Structure Analysis

The XRD diffractogram of pristine BCA (Figure 3) exhibited the typical reflections of cellulose Iα at 2θ ≈ 14.4˚ (1$\bar{1}$0), 16.8˚ (110), 22.6˚ (200) [47]. The diffraction peak at 2θ ≈ 26.5˚ detected in the acetylated bacterial cellulose derived from pineapple peel is suggested to be from silica/quartz residues rather than cellulose acetate itself. The most intense reflection of α-quartz is located at 2θ ≈ 26.6˚ (d ≈ 3.34 Å, hkl (101)), as reported in the ICDD/JCPDS database (PDF card No. 46-1045). This assignment is consistent with previous reports showing that pineapple peels contain biogenic silica nanoparticles that co-purify with nanocellulose extraction [48]. At the same time, sharp new reflections appeared at 2θ ≈ 31.7˚ and 36.2˚, corresponding to the (100) and (101) planes of wurtzite ZnO according to JCPDS card no. 36-1451) [49].

Using the Segal method, the crystallinity index (CrI) of BCA was calculated as 84.06%, confirming the highly ordered structure of cellulose (Table 1). Upon the incorporation of PVA and ZnO, notable changes were observed in the XRD profiles. The intensity of the (200) reflection increased for the 2.5 wt.% composite ($I_{(200)}$ = 827 vs. 577 for BCA), but the parallel rise in the amorphous background (I_{am} = 160 vs. 92) resulted in a net decrease in CrI to 80.65%. A further decrease to 79.51% was observed at 5.0 wt.% PVA/ZnO addition. The reduction of CI was observed in a carboxy methyl cellulose blend with PVA [50][51] and also in cotton linter [52]. The reduction in CrI demonstrates that PVA disrupts the ordered arrangement of cellulose fibrils, thereby expanding the amorphous fraction, by forming hydrogen bonds with cellulose hydroxyl groups [53]. The broadening of cellulose peaks in the composite diffractograms supports this interpretation. The increase in the amorphous region of films could be good for improving the toughness of the blend films. Interestingly, the 2.5 wt.% PVA/ZnO composite displayed the highest $I_{(200)}$ value, suggesting that moderate PVA loading may enhance the packing or orientation of cellulose microfibrils despite the overall reduction in CrI. By contrast, the 5.0 wt.% composite showed broader cellulose peaks, reflecting a stronger amorphous contribution. This implies that the balance between flexibility (from PVA) and reinforcement (from ZnO) can be tuned by controlling PVA content.

In this study, the crystallite size of cellulose (200) reflection around 2θ ≈ 22˚ was found to increase slightly from ~8.58 nm in BCA to ~8.60 nm in BCA/ZnO(2.5 wt.%)/PVA 2.5 wt.%, and further to ~9.36 nm in BCA/ZnO(2.5 wt.%)/PVA 5.0 wt.%. This trend aligns with previous reports in PVA-ZnO systems, in which elevating ZnO content leads to modest but measurable growth in average crystallite size for both ZnO and polymer phases. Abd-Elnaiem et al. [49] observed crystallite size increments in PVA-ZnO nanocomposites as ZnO

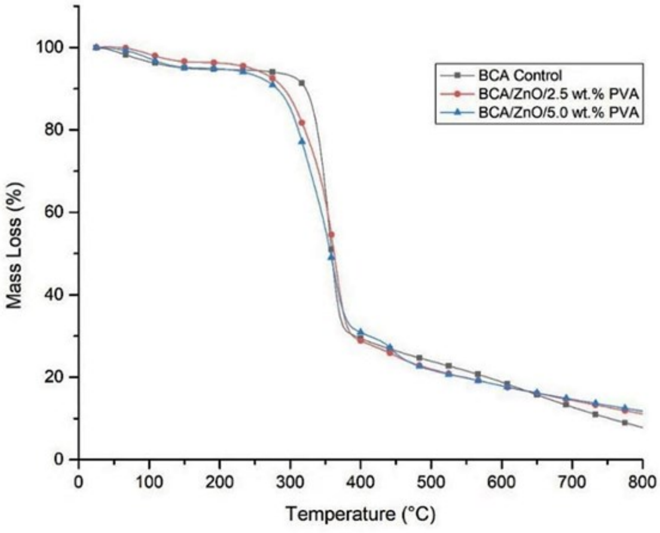

Figure 5. TGA analysis of BCA/ZnO/PVA membrane.

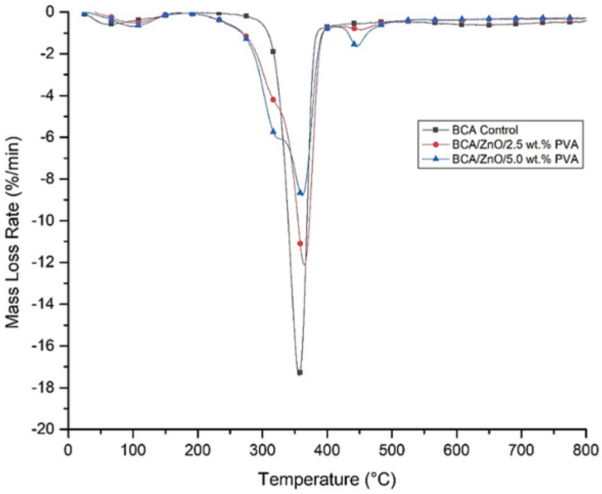

Figure 6. DTG analysis of BCA/ZnO/PVA membrane.

loading increased from 1 wt.% to 3 wt.%, paralleled by sharper ZnO diffraction peaks. The slight increase in crystallite size at BCA/ZnO(2.5 wt.%)/PVA 5.0 wt.% is attributed to PVA, which introduces strong hydrogen bonding with cellulose acetate chains, which reduces steric hindrance [54] and enhances chain mobility [55]. This allows the cellulose acetate chains to align more easily, favoring crystal growth over nucleation, and leading to the formation of fewer but larger crystalline domains.

3.3. Functional Group Analysis

The functional group analysis of BCA samples using FTIR was recorded at a wavenumber of 400 to 4000 cm^{-1}. They show a minor difference before and after adding PVA (Figure 4), as shown in Table 2. The incorporation of ZnO nanoparticles did not eliminate the characteristic bands of cellulose acetate and PVA but led to slight shifts and intensity changes, indicating possible hydrogen bonding and interfacial interactions between ZnO and the polymer matrix. Also, the distinct ZnO peaks were not clearly detected due to the relatively low concentration of ZnO, contributing only indirect effects on the FTIR spectrum.

The FTIR spectrum of BCA incorporated with PVA and ZnO revealed characteristic vibration bands of cellulose and its functional groups. The broad absorption band around 3500 cm^{-1} corresponds to the stretching vibration of hydroxyl (–OH) groups. Also, the peak at 1745 cm^{-1} is attributed to the carbonyl (C=O) stretching of the acetyl group [57]. Likewise, the band at 1650 cm^{-1} corresponds to –OH bending vibrations related to water adsorption, indicating the hydrophilic nature of cellulose [58]. In addition, the peak at 1446 cm^{-1} is assigned to symmetric bending of $–CH_2$ groups [59], which shifted to 1475 cm^{-1} after the addition of PVA, suggesting intermolecular interactions between PVA and cellulose acetate [60]. Moreover, the band at 1387 cm^{-1} is associated with –OH bending vibrations [61][62], while the absorption peak at 930 cm^{-1} corresponds to C–O stretching of the cellulose backbone [63][64].

3.4. Thermal Degradation Analysis

Figures 5 and 6 show the thermal degradation analysis of bagasse fiber using TGA curve, and the quantitative results are summarized in Table 3. It was observed that the membrane exhibits four stages of thermal degradation. Stage 1 starts at 25 ˚C and goes up to 200 ˚C, where devolatilization begins, which is associated with the release of light volatiles and moisture content [65]. Also, the membranes experienced a mass loss of 6.0% each and the mass loss at this stage is caused by water evaporation and hemicellulose decomposition. In addition, the material that has not completely evaporated will continue to stage 2 as the main thermal degradation.

Upon entering stage 2, which occurs between 200 ˚C and 400 ˚C, is the primary thermal degradation phase. Under these conditions, the control membrane degrades more slowly, starting to degrade at 267 ˚C. The peak degradation temperatures for the control membrane, the 2.5 wt.% and 5.0 wt.% PVA composite membranes were 356 ˚C, 363 ˚C, and 360 ˚C, with mass losses of 69.6%, 71.2%, and 69.1.8%, and the degradation rates of 17.4%/min, 12.0%/min, and 8.8%/min, respectively. Moreover, the addition of PVA reduces the mass loss rate during thermal degradation, indicating a slowdown in thermal decomposition. Interestingly, with the addition of 5.0 wt.% PVA, there was a deflection in the mass loss rate at 320 ˚C.

The stage 3 occurs between 400 ˚C and 500 ˚C and involves an additional decomposition phase where increasing PVA content results in an additional decomposition phase at 447 ˚C. The final decomposition phase happens at stage 4. Here, the degradation proceeds more slowly and involves the release of residual material not burned in the previous stage. However, the final phase produces ash residues of 7.8%, 11.2%, and 11.8% for the control membrane, membrane with 2.5 wt.% PVA addition, and PVA 5.0 wt.%. The addition of PVA can enhance the thermal stability of a material due to the presence of –OH groups in its and the polymer chains are able to form strong hydrogen bonds with other components, resulting in a denser network that restricts polymer chain mobility. This structural reinforcement increases the energy required to initiate thermal degradation. Moreover, PVA can act as a binder that improves particle dispersion within composites and strengthens interfacial bonding, thereby decelerating the rate of mass loss upon heating. Several studies have demonstrated this effect, as reported improved thermal stability in gelatin/starch/PVA composites based on TGA–DSC analysis [66], and improved thermal stability as relevant to previously reported in scaffold product [67].

3.5. Mechanical Properties

The mechanical properties of BCA/ZnO with the addition of PVA are as shown in Figure 7. Membrane BCA control, BCA/ZnO(0.25 wt%) with PVA 2.5 wt.% and 5.0 wt.% have tensile strength of 42.72 ± 14.53, 140.86 ± 26.70, and 139.34 ± 29.69 MPa, with elastic modulus of 3844 ± 738.15, 6613.56 ± 462.6, and 5050.41 ± 454.22 MPa, respectively. Adding PVA increases the tensile strength and elastic modulus of the membrane by

Table 3. Summary of TGA–DTG Results for BCA/ZnO/PVA Membranes.

Sample	**Peak Degradation Temperature (°C)**	**Total Mass Loss (%)**	**Degradation Rate (%/min)**	**Residue (%)**	**Remarks**
Control (BCA/ZnO(0.25 wt.%)	356	69.6	17.4	7.8	Highest degradation rate; least stable
BCA/ZnO(0.25 wt.%)/ PVA 2.5 wt.%	363	71.2	12.0	11.2	Improved stability; slower degradation
BCA/ZnO(0.25 wt.%)/ PVA 5.0 wt.%	360	69.8	8.8	11.8	Most thermally stable; lowest rate of mass loss

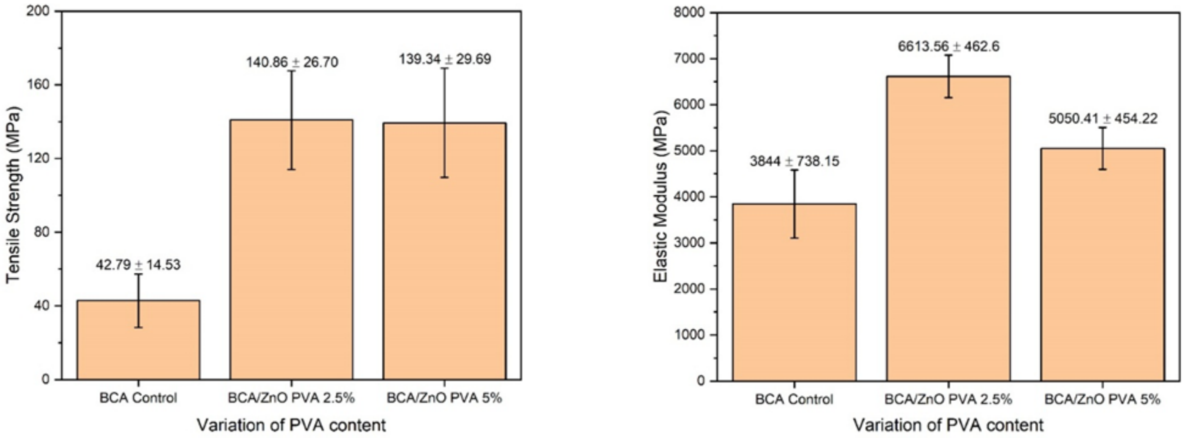

(A) **(B)**

Figure 7. Mechanical properties of BCA/ZnO with the addition of PVA membrane: (A) Tensile strength and (B) elastic modulus.

about 329% and 172%, respectively, at the addition of PVA of 2.5 wt.%.

Statistical analysis using one-way ANOVA identified that adding PVA to BCA membranes has a significant difference in the tensile strength (n =5, F-value of 26.223, $p < 0.05$) and elastic modulus (n =5, F-value of 26.223, $p < 0.05$). Post hoc analysis using the Tukey test indicates that adding 2.5 wt.% PVA and 5.0 wt.% PVA to the BCA membrane can significantly affect the tensile strength and elastic modulus of BCA membrane. However, the mechanical properties of BCA/ZnO with 0.25 wt.% PVA are not significantly different from BCA/ZnO with 0.25 wt.% PVA. On the other hand, PVA filled the empty spaces in BCA membrane, thereby increasing its mechanical strength as well as addition of 5.0 wt.% PVA results in a plasticizing effect that leads to a decrease in tensile strength.

In this case, PVA reacts with BCA membrane through resulting cross-linked hydrogen bonds (-OH) and C=O functional group (see Table 2), creating a denser and more stable polymer network (see Figure 2), improving stress transfer between components. In addition, the PVA also acts as a compatibilizing agent, distributing nanocellulose homogeneously within the CA matrix. The combination of these chemical and morphological effects significantly increases the tensile strength, and more PVA content reduces the elastic modulus of BCA/ZnO/PVA composite membrane, which means the membrane is more flexible. A similar result has been reported that PVA increases the mechanical properties of cellulose acetate membrane for lithium extraction from seawater [68] and increase the strain in Chitosan membrane up to 250% [69]. This indicates that cross-linking creates regular spacing between polymers, resulting in stronger interpolymer bonds. With these strong interpolymer forces, the membrane is less susceptible to damage from external forces.

3.7. Antibacterial Activity

Antibacterial activity of the membranes was evaluated against *E. coli* (Gram-negative) and *S. aureus* (Gram-positive) using the agar diffusion method (Figure 8, Table 4). The BCA membrane exhibited no inhibition zone against both *E. coli* and *S. aureus*. One-way ANOVA analysis indicates that the incorporation of ZnO/PVA into BCA matrix significantly improved the antibacterial properties compared with control membrane (P-value of 0.00 for *E. coli* and P-value of 0.005 for *S. aureus*). Moreover, the addition of PVA of 2.5 wt.% and 5.0 wt.% results in inhibition zones against *E. coli* of 8.07 ± 1.52 mm and 10.12 ± 2.19 mm, respectively. Similarly, inhibition zones against *S. aureus* reach 8.37 ± 3.28 mm and 8.84 ± 2.24 mm, respectively. Compared with the inhibition zone of chloramphenicol as a positive control, the composite membrane (with 5.0 wt.% PVA) had an inhibition zone of approximately 40.5% and 45.3% of the positive control for *S. aureus* and *E. coli*, respectively.

The difference in antibacterial activity between the two bacterial strains is due to *E. coli*, as a Gram-negative bacterium, which possesses an outer membrane composed of lipopolysaccharides and porin proteins, which play a critical role in determining susceptibility to antibacterial agents. Also, this outer membrane generally limits the penetration of metal ions, thereby reducing antibacterial efficiency. In contrast, *S. aureus*, as a Gram-positive bacterium, has a thicker but more permeable peptidoglycan layer without an outer membrane, which results in a different interaction pattern with metal nanoparticles [70]. Moreover, the interaction of ZnO nanoparticles causes stress responses, protein aggregation, and alters gene function related to metabolism, then disrupting cellular functions [71].

Although an inhibition zone was increased at BCA/ZnO/PVA membrane, post-hoc Tukey analysis revealed that the addition of PVA 2.5 wt.% and 5.0 wt.% was not statistically significantly different ($p > 0.05$) in inhibition zone. This indicates that the enhancement of antibacterial activity is primarily caused by the presence of ZnO nanoparticles rather than the addition of PVA. In addition, the dispersed ZnO particles also contribute to increased antibacterial properties, although the amount is relatively small [71]. Moreover, the ZnO imparts bactericidal effects through multiple mechanisms, including Zn^{2+} ion release, reactive oxygen species generation, and direct disruption of bacterial cell walls [72]. In this case, PVA mainly functions as a polymer stabilizer to ensure homogeneous dispersion of ZnO within the BCA matrix, but does not contribute directly to antibacterial activity. Practically, antibacterial activity function serves as a biofouling control mechanism, preventing the formation of bacterial biofilms that typically clog filtration systems.

3.8. Bacteria Filtration Performance

The membrane was applied for filtering the brackish water from the estuary in aquaculture environment. It was observed that the addition of PVA and ZnO to BCA membrane matrix increased the efficiency of microorganism removal and strengthened the membrane structure. In the pure

(A) (B)

Figure 8. Antibacterial activity BCA (I), BCA/ZnO(0.25 wt%)/PVA2.5wt.% (II), and BCA/ZnO(0.25 wt%)/PVA 5% using (A) *S. aureus* and (B) *E. coli*.

Table 4. Inhibition activity of membrane against *E. coli* and *S. aureus*.

Samples	Halo diameter (mm)	
	E. coli	*S. aureus*
Control (+)	22.32	21.85
BCA	0.00^a	0.00^a
BCA/ZnO(0.25 wt.%)/PVA2.5wt.%	8.07 ± 1.52^b	8.37 ± 3.28^b
BCA/ZnO(0.25 wt.%)/PVA5.0wt.%	10.12 ± 2.19^b	8.84 ± 2.24^b

Notes: Similar notation of a,b,c means the treatment is not significantly different

Table 5. Bacterial filtration test for the developed membrane.

Membrane type	**Abundance of bacteria (CFU/mL)**	**LRV**	**Bacteria dominant**
BCA (control)	2.85×10^9	-	*Pseudomonas, Aeromonas, Proteus*
BCA/ZnO(0.25 wt.%)/ PVA 2.5 wt.%	1.59×10^8	1.25	*Micrococcus, Bacillus*
BCA/ZnO(0.25 wt.%)/ PVA 5.0 wt.%	2.63×10^8	1.03	*Bacillus, Lactobacillus, Corynebacterium*

BCA membrane (control), the bacterial abundance after filtration was recorded at approximately 2.85 × 10^9 CFU/mL (Table 5), indicating that the membrane still has pores large enough to allow some microorganisms to pass through. After modification with the addition of ZnO and PVA of 2.5 wt.% and 5.0 wt.%, the bacterial abundance decreased sharply to 1.59 × 10^8 CFU/mL and 2.63 × 10^8 CFU/mL, with LRV values of 1.25 and 1.03, respectively. LRV value indicates the effectiveness of the filtration process increases 17.9 times compared to the control for BCA/ZnO/PVA 2.5 wt.% membrane and 10.7 times compared to the control for BCA/ZnO/PVA 5.0 wt.% membrane. This effectiveness data indicates that PVA plays an important role in increasing an effective filtration membrane through strengthening the intermolecular network of cellulose acetate through the formation of hydrogen bonds between the –OH groups of PVA and the acetyl groups of BCA, resulting in a denser and more uniform membrane structure. The addition of PVA to membranes affects the inner membranes' porosity and pore dimensions [73]. It is more emphasized by Razmgar and Nasirae [74] that the porosity of membranes decreased with an increase in PVA loading. So, in this case, at higher PVA concentrations (5%), it suggests the results in morphological irregularities and the formation of microchannels in some areas of the membrane. This allows some bacteria to pass through areas of low density, increasing post-filtration bacterial abundance. Moreover, the irregularity in surface morphology is also described by Razmgar and Nasiraee [74] which confirm the formation of irregularities and a granular surface in the membrane.

4. CONCLUSIONS

This study successfully synthesized the bacterial cellulose acetate (BCA) membranes derived from pineapple biowaste modified with PVA/ZnO nanoparticles and demonstrated their characteristics and functionality as a bacterial filtration membrane for aquaculture environment. Morphology analysis using SEM revealed that the BCA membrane exhibited a smooth and homogeneous fibril network, while the addition of PVA increased inter-fiber bonding and surface densification. At 2.5

wt.% PVA, the membrane maintained a visible fibrillar structure with improved compactness, whereas at 5.0 wt.% PVA, fibers appeared partially covered by a thin layer, producing a smoother surface. Structure analysis using XRD showed crystallinity index reduced from 84.06% (BCA control) to 80.65% (BCA/ZnO(0.25 wt.%)/PVA 2.5 wt.%) and 79.51% (BCA/ZnO(0.25 wt.%)/PVA 5.0 wt.%). The crystalline size increases from 8.58 nm to 9.36 nm. Besides, the addition of PVA is known to increase the mechanical properties by 329% and also the thermal stability of membrane. These results confirm that PVA disrupts the ordered arrangement of cellulose fibrils, enhances amorphous regions, and improves flexibility and thermal stability by reducing the degradation rate to 8.8%/min. Also, the ZnO at 0.25 wt.% dispersed well within the matrix and contributed significantly to antibacterial activity against *E. coli* and *S. aureus*. Additionally, the brackish water filtration tests showed decreases in bacterial abundance, with the addition of PVA 2.5 wt.% and 5.0 wt.% increasing the efficacy of bacterial filtration by 17.9 and 10.7 times, respectively. These results demonstrate how PVA and ZnO work together to enhance filtration capacity, mechanical stability, and antibacterial activity. However, as this study focused on specific composition ratios, the current reaction conditions are not yet fully optimized. Nevertheless, the research is restricted to short-term testing and laboratory-scale experiments with a single ZnO concentration. It is still necessary to investigate long-term durability, fouling resistance, fabrication scalability, and performance under various aquaculture conditions. To further the practical use of PVA/ZnO-modified BCA membranes in sustainable water treatment, future research should conduct comprehensive optimization of reaction conditions and nanoparticle loading, evaluate field performance, and assess continuous operation.

AUTHOR INFORMATION

Corresponding Author

Heru Suryanto — Department of Mechanical and Industrial Engineering, Universitas Negeri Malang, Malang-65145 (Indonesia);
orcid.org/0000-0001-7037-1868
Email: heru.suryanto.ft@um.ac.id

Authors

Uun Yanuhar — Department of Aquatic Resources Management, Brawijaya University, Malang-65145 (Indonesia);
orcid.org/0000-0003-3360-8752

Joseph Selvi Binoj — Department of Mechanical Engineering, Alasala Colleges, Dammam-31483 (Kingdom of Saudi Arabia);
orcid.org/0000-0002-7222-4463

Leong-Seng Lim — Department of Aquatic Resources Management, Brawijaya University, Malang-65145 (Indonesia); Borneo Marine Research Institute, Universiti Malaysia Sabah, Sabah-88400 (Malaysia);
orcid.org/0000-0002-0404-1083

Arumugam Kumaravel — Department of Mechanical Engineering, K.S.Rangasamy College of Technology, Tiruchengode – 637215 (India);
orcid.org/0000-0002-7624-9748

Aminnudin Aminnudin — Department of Mechanical and Industrial Engineering, Universitas Negeri Malang, Malang-65145 (Indonesia);
orcid.org/0000-0002-3883-0136

Fajar Nusantara — Department of Mechanical and Industrial Engineering, Universitas Negeri Malang, Malang-65145 (Indonesia);
orcid.org/0009-0002-7062-0646

Defa Rizqi Machfuda — Master of Aquaculture Study Program, Brawijaya University, Malang-65145 (Indonesia);
orcid.org/0009-0009-8964-8252

Komarudin Komarudin — Department of Mechanical and Industrial Engineering, Universitas Negeri Malang, Malang-65145 (Indonesia);
orcid.org/0000-0001-8854-9206

Aulia Surya Ramadhan — Program Study of Environmental Engineering, Brawijaya University, Malang-65145 (Indonesia);
orcid.org/0009-0002-0774-315X

Author Contributions

U. Y.: Conceptualization; Methodology; Data curation. H. S.: Funding acquisition; Writing - Original draft preparation. J. S. B.: Methodology;

Visualization. L.-S. L.: Supervision, Visualization. A. K.: Formal analysis, Writing - Review & Editing. A. A.: Writing - Reviewing and Editing. D. R. M.: Project administration, Resources. F. N.: Formal analysis, Writing - Review & Editing, K. K.: Formal analysis, Writing - Review & Editing. A. S. R.: Formal analysis, Visualization.

Conflicts of Interest

The authors declare no conflict of interest.

ACKNOWLEDGEMENT

Many thanks are delivered to LPPM-UM and DPPM Dikti for funding the scheme of the Fundamental Research grant with a contract number of 2.6.153/UN32.14.1/LT/2025.

DECLARATION OF GENERATIVE AI

Authors declare that this article is the original work of the author without using AI tools for writing sentences and/or creating/editing tables and figures in this manuscript.

REFERENCES

[1] Z. Liu, R. Zhao, X. Zhang, H. Wang, C. Zhang, J. Liu, and P. Zhu. (2025). "Comparison of Bacterial Cellulose Production by Various Biomass Wastes as Culture Media". *International Journal of Biological Macromolecules.* **309** : 143091. 10.1016/j.ijbiomac.2025.143091.

[2] X. Wang, J. Chen, G. Yang, Q. Zheng, Y. Zheng, and L. Wang. (2026). "Comparative Chemical Profiling of Callus and Seeds of Theobroma cacao by Precolumn Derivatization GC-MS and LC-MS". *Research Square.* 10.21203/rs.3.rs-8390136/v1.

[3] T. Aziz, A. Farid, F. Haq, M. Kiran, A. Ullah, K. Zhang, C. Li, S. Ghazanfar, H. Sun, R. Ullah, A. Ali, M. Muzammal, M. Shah, N. Akhtar, S. Selim, N. Hagagy, M. Samy, and S. K. Al Jaouni. (2022). "A Review on the Modification of Cellulose and Its Applications". *Polymers.* **14** : 3206. 10.3390/polym14153206.

[4] D. R. Ningrum, S. N. S. Yuliandini, F. N. Abrar, A. Surwadinata, Z. Sapak, A. Çelik, A. Soffan, and A. I. Santosa. (2025). "Genetic diversity of pineapple mealybug wilt-associated virus-1 and -2, and Dysmicoccus spp. vectors in Java Island, Indonesia". *Tropical Plant Pathology.* **50** (1). 10.1007/s40858-025-00752-x.

[5] P. K. Sarangi, T. A. Singh, N. J. Singh, K. P. Shadangi, R. K. Srivastava, A. K. Singh, A. K. Chandel, N. Pareek, and V. Vivekanand. (2022). "Sustainable Utilization of Pineapple Wastes for Production of Bioenergy, Biochemicals and Value-Added Products: A Review". *Bioresource Technology.* **351** : 127085. 10.1016/j.biortech.2022.127085.

[6] S. K. Bhatia, S. Mehariya, R. K. Bhatia, M. Kumar, A. Pugazhendhi, M. K. Awasthi, A. E. Atabani, G. Kumar, W. Kim, S. O. Seo, and Y. H. Yang. (2021). "Wastewater Based Microalgal Biorefinery for Bioenergy Production: Progress and Challenges". *Science of the Total Environment.* **751** : 141599. 10.1016/j.scitotenv.2020.141599.

[7] H. V. Le, N. T. Dao, H. T. Bui, P. T. K. Le, K. A. Le, A. T. T. Tran, K. D. Nguyen, H. H. M. Nguyen, and P. H. Ho. (2023). "Bacterial Cellulose Aerogels Derived from Pineapple Peel Waste for the Adsorption of Dyes". *ACS Omega.* **8** (37): 33412-33425. 10.1021/acsomega.3c03130.

[8] A. D. M. de Medeiros, C. J. G. da Silva Junior, J. D. P. de Amorim, H. A. do Nascimento, A. Converti, A. F. de S. Costa, and L. A. Sarubbo. (2021). "Biocellulose for Treatment of Wastewaters Generated by Energy Consuming Industries: A Review". *Energies.* **14** (16): 5066. 10.3390/en14165066.

[9] M. Kaczmarek, M. Jędrzejczak-Krzepkowska, and K. Ludwicka. (2022). "Comparative Analysis of Bacterial Cellulose Membranes Synthesized by Chosen Komagataeibacter Strains and Their Application Potential". *International Journal of Molecular Sciences.* **23** (6): 3391. 10.3390/ijms23063391.

[10] L. Zhao, Y. Ma, M. K. Awasthi, D. Tian, J. He, M. Huang, J. Zou, Y. Lei, and F. Shen.

(2025). "Enhancement of Bacterial Cellulose Production Synergistic H2 and Volatile Fatty Acids from Fruit and Vegetable Waste through Retting Pretreatment". *Industrial Crops And Products.* **225** : 120554. 10.1016/j.indcrop.2025.120554.

[11] T. Mahsuli, A. Larasati, A. Aminnudin, and J. Maulana. (2023). "Effect of the Homogenization Process on Titanium Oxide-Reinforced Nanocellulose Composite Membranes". *Journal of Mechanical Engineering Science and Technology (JMEST).* **7** (2). 10.17977/um016v7i22023p137.

[12] Y. Liu, H. Liu, S. Guo, Y. Zhao, J. Qi, R. Zhang, J. Ren, H. Cheng, M. Zong, X. Wu, and B. Li. (2024). "A review of carbon nanomaterials/bacterial cellulose composites for nanomedicine applications". *Carbohydrate Polymers.* **323** : 121445. 10.1016/j.carbpol.2023.121445.

[13] G. Alfassi, D. M. Rein, A. Shpigelman, and Y. Cohen. (2019). "Partially Acetylated Cellulose Dissolved in Aqueous Solution: Physical Properties and Enzymatic Hydrolysis". *Polymers (Basel).* **11** (11). 10.3390/polym11111734.

[14] T. Esser, T. Wolf, T. Schubert, J. Benra, S. Forero, G. Maistros, S. Barbe, G. V. Theodorakopoulos, D. S. Karousos, A. A. Sapalidis, and E. P. Favvas. (2021). "CO(2)/CH(4) and He/N(2) Separation Properties and Water Permeability Valuation of Mixed Matrix MWCNTs-Based Cellulose Acetate Flat Sheet Membranes: A Study of the Optimization of the Filler Material Dispersion Method". *Nanomaterials (Basel).* **11** (2). 10.3390/nano11020280.

[15] U. Yanuhar, H. Suryanto, S. A. Sardjono, I. K. Ningrum, A. Aminnudin, and J. S. Binoj. (2022). "Effect of Titanium Dioxide Nanoparticle on Properties of Nanocomposite Membrane Made of Bacterial Cellulose". *Journal of Natural Fibers.* **19** (16): 13914-13927. 10.1080/15440478.2022.2112797.

[16] A. C. Mecha, M. N. Chollom, B. F. Babatunde, E. K. Tetteh, and S. Rathilal. (2023). "Versatile Silver-Nanoparticle-Impregnated Membranes for Water Treatment: A Review". *Membranes.* **13** (4): 432. 10.3390/membranes13040432.

[17] L. d. C. Alves, M. A. Cerqueira, M. A. González-Goméz, P. Garcia-Acevedo, Á. A. Prieto, Y. Piñeiro Redondo, L. Pastrana, and J. Rivas. (2024). "Innovative Films by Embedding Magnetic Nanoparticles in Cellulose Acetate". *Food Packaging and Shelf Life.* **42** : 101264. 10.1016/j.fpsl.2024.101264.

[18] E. Kumi, V. R. Veeredhi, and C. Enweremadu. (2024). "Innovative Approaches for Improving ORC Performance: A Review of Pure Fluids, Zeotropic Mixtures, and Nanoparticles". *Journal of Mechanical Engineering Science and Technology (JMEST).* **8** (2). 10.17977/10.17977/um016v8i22024p253.

[19] L. Yu and A. L. Skov. (2017). "ZnO as a Cheap and Effective Filler for High Breakdown Strength Elastomers". *RSC Advances.* **7** : 45784-45791. 10.1039/C7RA09479E.

[20] N. Asif, M. Amir, and T. Fatma. (2023). "Recent Advances in the Synthesis, Characterization and Biomedical Applications of Zinc Oxide Nanoparticles". *Bioprocess and Biosystems Engineering.* **46** : 1377-1398. 10.1007/s00449-023-02886-1.

[21] O. Ejiohuo, H. Onyeaka, A. Akinsemolu, O. F. Nwabor, K. F. Siyanbola, P. Tamasiga, and Z. T. Al-Sharify. (2025). "Ensuring Water Purity: Mitigating Environmental Risks and Safeguarding Human Health". *Water Biology and Security.* **4** : 100341. 10.1016/j.watbs.2024.100341.

[22] J. Cevallos-Mendoza, C. G. Amorim, J. M. Rodríguez-Díaz, and M. d. C. B. S. M. Montenegro. (2022). "Removal of Contaminants from Water by Membrane Filtration: A Review". *Membranes.* **12** (6): 570. 10.3390/membranes12060570.

[23] N. S. Zain, M. H. H. Mahmoud, M. I. Khan, F. Zafar, S. Manzoor, N. Akhtar, M. A. Khan, I. H. El Azab, and Z. M. El-Bahy. (2024). "Machine Learning-Assisted Optimization and Evaluation of Methylene Blue Adsorption Kinetics on Citrus aurantifolia Leaves: Insights from Isotherm

and Thermodynamic Studies". *Journal of the Taiwan Institute of Chemical Engineers.* **164** : 105696. 10.1016/j.jtice.2024.105696.

[24] A. A. Alves, W. E. Silva, M. F. Belian, L. S. G. Lins, and A. Galembeck. (2020). "Bacterial Cellulose Membranes for Environmental Water Remediation and Industrial Wastewater Treatment". *International Journal of Environmental Science and Technology.* **17** (9): 3997-4008. 10.1007/s13762-020-02746-5.

[25] K. Sharma, P. Choudhary, A. Majeed, S. Guleria, M. Kumar, A. K. Rana, and G. Rajauria. (2025). "Cellulose Based Membranes, Hydrogels and Aerogels for Water Treatment Application". *Industrial Crops And Products.* **225** : 120474. 10.1016/j.indcrop.2025.120474.

[26] P. Grzybek, G. Dudek, and B. van der Bruggen. (2024). "Cellulose-Based Films and Membranes: A Comprehensive Review on Preparation and Applications". *Chemical Engineering Journal.* **495** : 153500. 10.1016/j.cej.2024.153500.

[27] B. Gul, E. Pekgenc, V. Vatanpour, and I. Koyuncu. (2023). "A Review of Cellulose-Based Derivatives Polymers in Fabrication of Gas Separation Membranes: Recent Developments and Challenges". *Carbohydrate Polymers.* **321** : 121296. 10.1016/j.carbpol.2023.121296.

[28] Z. Li, F. Qiu, X. Yue, Q. Tian, D. Yang, and T. Zhang. (2021). "Eco-Friendly Self-Crosslinking Cellulose Membrane with High Mechanical Properties from Renewable Resources for Oil/Water Emulsion Separation". *Journal of Environmental Chemical Engineering.* **9** :105857. 10.1016/j.jece.2021.105857.

[29] B. Hudaib, Z. Al-Qodah, R. Abu-Zurayk, H. Waleed, and W. Omar. (2024). "Fabrication of Blended Cellulose Acetate/Poly-Pyrrole Ultrafiltration Membranes for Crude Oil Wastewater Separation". *Case Studies in Chemical and Environmental Engineering.* **9** : 100692. 10.1016/j.cscee.2024.100692.

[30] X. Shao, G. Yao, Z. Wang, Y. Chen, D. Yang, F. Qiu, and T. Zhang. (2024). "MOFs and Surface Modification Synergistically Modulated Cellulose Membranes for Enhanced Water Permeability and Efficient Tellurium Separation in Wastewater". *Journal of Cleaner Production.* **434** : 139873. 10.1016/j.jclepro.2023.139873.

[31] R. Weng, G. Chen, X. He, J. Qin, S. Dong, J. Bai, S. Li, and S. Zhao. (2024). "The Performance of Cellulose Composite Membranes and Their Application in Drinking Water Treatment". *Polymers.* **16** (2): 285. 10.3390/polym16020285.

[32] L. Zhang, S. Zheng, Z. Hu, L. Zhong, Y. Wang, X. Zhang, and J. Xue. (2020). "Preparation of Polyvinyl Alcohol/Bacterial-Cellulose-Coated Biochar-Nanosilver Antibacterial Composite Membranes". *Applied Sciences.* **10** (3): 752. 10.3390/app10030752.

[33] S. Huang, X. Wang, Y. Zhang, Y. Meng, F. Hua, and X. Xia. (2022). "Cellulose Nanofibers/Polyvinyl Alcohol Blends as an Efficient Coating to Improve the Hydrophobic and Oleophobic Properties of Paper". *Scientific Reports.* **12** (1): 16148. 10.1038/s41598-022-20499-8.

[34] S. Elarbaoui. (2025). "The Integrated Zinc Oxide Nanoparticle Membranes for Wastewater Treatment". *Polish Journal of Environmental Studies.* **34** (3): 2103-2115. 10.15244/pjoes/187776.

[35] S. Ladhari, N. N. Vu, J. V. Bastien, B. V. Tran, T. H. Nguyen, A. Saidi, S. Barnabe, C. Sollogoub, and P. Nguyen-Tri. (2025). "A Green Synthesis Route of ZnO/Polyhydroxybutyrate Composites with Antibacterial and Biodegradable Properties". *Polymer Engineering and Science.* **65** (3): 1037-1054. 10.1002/pen.27055.

[36] N. R. Amasda, H. Suryanto, U. Yanuhar, F. Nusantara, and Q. A. Sias. (2025). "Surface Analysis of Bacterial Cellulose Membrane Made from Biowaste Added with ZnO Nanopowder". *Journal of Mechanical Engineering Science and Technology.* **9** (1): 281-290. 10.17977/um016v9i12025p281.

[37] S. Asadpour, A. Raeisi Vanani, M. Kooravand, and A. Asfaram. (2022). "A Review on Zinc Oxide/Poly(Vinyl Alcohol) Nanocomposites: Synthesis, Characterization

and Applications". *Journal of Cleaner Production.* **362** : 132297. 10.1016/j.jclepro.2022.132297.

[38] T. Mahsuli, H. Suryanto, A. Larasati, and M. Muhajir, "Mechanical Properties of Bacterial Nanocellulose Membrane from Pineapple Peel Waste after Homogenization Process," presented at the AIP Conference Proceedings, 2019. [Online]. Available: 10.1063/1.5115695.

[39] U. Yanuhar, H. Suryanto, M. Amin, J. Maulana, M. T. Mohamad Lal, and N. R. Caesar. (2024). "The Impact of Copper Oxide Nanoparticles Reinforced Nanocellulose Acetate Membrane on Antibacterial and Dye Removal Potency". *Results in Engineering.* **23** : 102788. 10.1016/j.rineng.2024.102788.

[40] U. Yanuhar, H. Suryanto, A. Aminnudin, H. W. Wijaya, J. Maulana, and N. R. Caesar. (2024). "Utilization of Pineapple Peel Waste/ZnO Nanoparticles Reinforcement for Cellulose-Based Nanocomposite Membrane and Its Characteristics". *Journal of Polymers and the Environment.* **32** (8): 3749-3764. 10.1007/s10924-024-03205-9.

[41] Y. T. Xiao, W. L. Chin, and S. B. Abd Hamid. (2015). "Facile Preparation of Highly Crystalline Nanocellulose by Using Ionic Liquid". *Advanced Materials Research.* **1087** : 106-110. 10.4028/www.scientific.net/AMR.1087.106.

[42] K. Domagała, J. Bell, N. S. Yüzbasi, B. Sinnet, D. Kata, and T. Graule. (2021). "Virus Removal from Drinking Water Using Modified Activated Carbon Fibers". *RSC Advances.* **11** (50): 31547-31556. 10.1039/D1RA06373A.

[43] M. D. Islam, F. J. Uddin, T. U. Rashid, and M. Shahruzzaman. (2023). "Cellulose Acetate-Based Membrane for Wastewater Treatment-A State-of-the-Art Review". *Materials Advances.* **4** : 4054-4102. 10.1039/D3MA00255A.

[44] A. Mocanu, G. Isopencu, C. Busuioc, O. M. Popa, P. Dietrich, and L. Socaciu-Siebert. (2019). "Bacterial Cellulose Films with ZnO Nanoparticles and Propolis Extracts: Synergistic Antimicrobial Effect". *Scientific Reports.* **9** : 17687. 10.1038/s41598-019-54118-w.

[45] O. Azhar, Z. Jahan, F. Sher, M. B. K. Niazi, S. J. Kakar, and M. Shahid. (2021). "Cellulose Acetate-Polyvinyl Alcohol Blend Hemodialysis Membranes Integrated with Dialysis Performance and High Biocompatibility". *Materials Science And Engineering: C.* **126** : 112127. 10.1016/j.msec.2021.112127.

[46] V. Vatanpour, S. Faghani, R. Keyikoglu, and A. Khataee. (2021). "Enhancing the Permeability and Antifouling Properties of Cellulose Acetate Ultrafiltration Membrane by Incorporation of ZnO@Graphitic Carbon Nitride Nanocomposite". *Carbohydrate Polymers.* **256** : 117413. 10.1016/j.carbpol.2020.117413.

[47] Z. Ling, S. Chen, X. Zhang, K. Takabe, and F. Xu. (2017). "Unraveling Variations of Crystalline Cellulose Induced by Ionic Liquid and Their Effects on Enzymatic Hydrolysis". *Scientific Reports.* **7** : 10230. 10.1038/s41598-017-09885-9.

[48] Y. R. Corrales-Ureña, C. Villalobos-Bermúdez, R. Pereira, M. Camacho, E. Estrada, O. Argüello-Miranda, and J. R. Vega-Baudrit. (2018). "Biogenic Silica-Based Microparticles Obtained as a Sub-Product of the Nanocellulose Extraction Process from Pineapple Peels". *Scientific Reports.* **8** : 10417. 10.1038/s41598-018-28444-4.

[49] N. Sedefoglu. (2023). "Characterization and Photocatalytic Activity of ZnO Nanoparticles by Green Synthesis Method". *Optik.* **288** : 171217. 10.1016/j.ijleo.2023.171217.

[50] M. A. Saadiah, D. Zhang, Y. Nagao, S. K. Muzakir, and A. S. Samsudin. (2019). "Reducing Crystallinity on Thin Film Based CMC/PVA Hybrid Polymer for Application as a Host in Polymer Electrolytes". *Journal of Non-Crystalline Solids.* **511** : 201-211. 10.1016/j.jnoncrysol.2018.11.032.

[51] A. M. Alghamdi. (2025). "Fabrication and Comprehensive Characterization of HPMC/PVA/CMC-MoO3 Bio-Nanocomposites: Enhanced Mechanical, Electrical, and Antibacterial Properties for Food Packaging Applications". *International Journal of Biological Macromolecules.* **287** : 138612.

10.1016/j.ijbiomac.2024.138612.

[52] A. Abdulkhani, E. Hojati Marvast, A. Ashori, Y. Hamzeh, and A. N. Karimi. (2013). "Preparation of Cellulose/Polyvinyl Alcohol Biocomposite Films Using 1-n-Butyl-3-Methylimidazolium Chloride". *International Journal of Biological Macromolecules.* **62** : 379-386. 10.1016/j.ijbiomac.2013.08.050.

[53] S. Nasibi, H. Nargesi Khoramabadi, M. Arefian, M. Hojjati, I. Tajzad, A. Mokhtarzade, M. Mazhar, and A. Jamavari. (2020). "A Review of Polyvinyl Alcohol/ Carboxymethyl Cellulose (PVA/CMC) Composites for Various Applications". *Journal of Composites and Compounds.* **2** 68 -75. 10.29252/jcc.2.2.2.

[54] H. Wang, Z. Shao, K. Shen, B. Bateer, F. Ren, and X. Qi. (2025). "Super Hydrophobic UHMWPE/PTFE/PVA Composites with Low Friction: Preparation and Wear Mechanism". *Polymers.* **17** (12): 1664. 10.3390/polym17121664.

[55] W. Fei, Z. Wu, H. Cheng, Y. Xiong, W. Chen, and L. Meng. (2023). "Molecular Mobility and Morphology Change of Poly (Vinyl Alcohol) (PVA) Film as Induced by Plasticizer Glycerol". *Journal of Polymer Science.* **61** (17): 1959-1970. 10.1002/pol.20230107.

[56] L. P. Alves, K. d. S. Oliveira, A. C. G. dos Santos, D. F. de Melo, L. M. C. d. C. Moreira, J. A. Oshiro Junior, D. T. C. da Silva, A. L. d. M. Cavalcanti, and B. P. G. d. L. Damasceno. (2024). "Cellulose Acetate Microparticles Synthesized from Agave sisalana Perrine for Controlled Release of Simvastatin". *Polymers.* **16** (13): 1898. 10.3390/polym16131898.

[57] M. Nasir, A. Subhan, B. Prihandoko, and T. Lestariningsih. (2017). "Nanostructure and Property of Electrospun SiO2-Cellulose Acetate Nanofiber Composite by Electrospinning". *Energy Procedia.* **107** : 227 -231. 10.1016/j.egypro.2016.12.133.

[58] S. Sharma, I. N. Najar, A. Radha, N. Nekkala, V. Sharma, and V. Kumar. (2025). "An Effective Method for Developing Cellulose-Based Polymer from Spent Lemongrass for Use as Packaging Material". *Biomass Conversion and Biorefinery.* 10.1007/s13399-025-06607-4.

[59] N. Thanarattanasap, P. Tumawong, T. Sinsawat, E. Chaichana, and B. Jongsomjit. (2019). "Polyethylene/Bacterial-Cellulose Biocomposite Synthesized via In Situ Polymerization with Zirconocene/MMAO Catalyst". *Engineering Journal.* **23** (3): 15-28. 10.4186/ej.2019.23.3.15.

[60] R. E. Elwardany, H. Shokry, A. A. Mustafa, and A. E. Ali. (2023). "Influence of the Prepared Activated Carbon on Cellulose Acetate for Malachite Green Dye Removal from Aqueous Solution". *Macromolecular Research.* **31** (11): 1043-1060. 10.1007/s13233-023-00187-w.

[61] N. Thongwai, W. Futui, N. Ladpala, B. Sirichai, A. Weechan, J. Kanklai, and P. Rungsirivanich. (2022). "Characterization of Bacterial Cellulose Produced by Komagataeibacter maltaceti P285 Isolated from Contaminated Honey Wine". *Microorganisms.* **10** : 528. 10.3390/microorganisms10030528.

[62] H. Yu, A. Lanot, and N. Mao. (2024). "The Relationship between Molecular Weight of Bacterial Cellulose and the Viscosity of Its Copper (II) Ethylenediamine Solutions". *Cellulose.* **31** (13): 7973-7992. 10.1007/s10570-024-06106-1.

[63] S. Dinant, N. Wolff, F. De Marco, F. Vilaine, L. Gissot, E. Aubry, C. Sandt, C. Bellini, and R. Le Hir. (2019). "Synchrotron FTIR and Raman Spectroscopy Provide Unique Spectral Fingerprints for Arabidopsis Floral Stem Vascular Tissues". *Journal of Experimental Botany.* **70** (3): 871-884. 10.1093/jxb/ery396.

[64] T. Jeoh, J. D. Nill, W. Zhao, S. R. Narayanasamy, L. Chen, and H. Y. N. Holman. (2024). "Spatiotemporal Dynamics of Cellulose during Enzymatic Hydrolysis Studied by Infrared Spectromicroscopy". *Green Chemistry.* **26** (1): 396-411. 10.1039/D3GC03279E.

[65] Sukarni, Sumarli, P. Puspitasari, H. Suryanto, and R. F. Wati, "Physicochemical Characteristics of Various Inorganic Combustible Solid Waste (ICSW) Mixed as

Sustainable Solid Fuel," presented at the AIP Conference Proceedings, 2017. [Online]. Available: 10.1063/1.5003549.

[66] D. Qiao, Y. Huang, X. Hou, F. Ye, K. Wu, F. Jiang, G. Zhao, B. Zhang, and F. Xie. (2024). "Enhancing Thermal Stability and Mechanical Resilience in Gelatin/Starch Composites through Polyvinyl Alcohol Integration". *Carbohydrate Polymers.* **344** : 122528. 10.1016/j.carbpol.2024.122528.

[67] A. Allafchian, S. Saeedi, and S. A. H. Jalali. (2022). "Biocompatibility of Electrospun Cell Culture Scaffolds Made from Balangu Seed Mucilage/PVA Composites". *Nanotechnology.* **33** (7): 075302. 10.1088/1361-6528/ac3860.

[68] Z. Qiu, M. Wang, Y. Chen, T. Zhang, D. Yang, and F. Qiu. (2021). "Li4Mn5O12 Doped Cellulose Acetate Membrane with Low Mn Loss and High Stability for Enhancing Lithium Extraction from Seawater". *Desalination.* **506** : 115003. 10.1016/j.desal.2021.115003.

[69] R. A. Lusiana, V. D. A. Sangkota, and S. J. Santosa. (2018). "Chitosan Succinate/PVA-PEG Membrane: Preparation, Characterization and Permeation Ability Test on Creatinine". *Jurnal Kimia Sains dan Aplikasi.* **21** (2): 80-84. 10.14710/jksa.21.2.80-84.

[70] I. Ghai. (2023). "A Barrier to Entry: Examining the Bacterial Outer Membrane and Antibiotic Resistance". *Applied Sciences.* **13** (7): 4238. 10.3390/app13074238.

[71] K. M. Amin, A. M. Partila, H. A. Abd El-Rehim, and N. M. Deghiedy. (2020). "Antimicrobial ZnO Nanoparticle-Doped Polyvinyl Alcohol/Pluronic Blends as Active Food Packaging Films". *Particle & Particle Systems Characterization.* **37** (4): 2000006. 10.1002/ppsc.202000006.

[72] B. L. da Silva, M. P. Abuçafy, E. B. Manaia, J. A. O. Junior, B. G. Chiari-Andréo, R. C. L. R. Pietro, and L. A. Chiavacci. (2019). "Relationship between Structure and Antimicrobial Activity of Zinc Oxide Nanoparticles: An Overview". *International Journal of Nanomedicine.* **14** : 9395-9410. 10.2147/IJN.S216204.

[73] M. E. Talukder, M. N. Pervez, H. Song, A. Buonerba, G. K. Stylios, V. Naddeo, W. Kujawski, and A. Figoli. (2025). "Eco-Friendly Synthesis of Porous and Charged Polyethersulfone Membrane for Improved Protein Separation Efficiency". *Results in Engineering.* **25** : 104422. 10.1016/j.rineng.2025.104422.

[74] K. Razmgar and M. Nasiraee. (2022). "Polyvinyl Alcohol-Based Membranes for Filtration of Aqueous Solutions: A Comprehensive Review". *Polymer Engineering and Science.* **62** (1): 25-43. 10.1002/pen.25846.